Published in Sensors and Actuators A: Physical 148, issue 2, 416-421, 2008
which should be used for any reference to this work

Microhotplates with TiN heaters

J.F. Creemer [a,c,*], D. Briand [b], H.W. Zandbergen [c], W. van der Vlist [a], C.R. de Boer [a], N.F. de Rooij [b], P.M. Sarro [a]

[a] DIMES-ECTM (Delft Institute of Microsystems and Nanoelectronics), Delft University of Technology, PO Box 5053, 2600 GB Delft, Netherlands
[b] Institute of Microtechnology, University of Neuchâtel, rue Jaquet-Droz 1, P.O. Box 526, CH-2002 Neuchâtel, Switzerland
[c] High Resolution Electron Microscopy, Kavli Institute of NanoScience, Delft University of Technology, Lorentzweg 1, 2628 CJ Delft, Netherlands

ABSTRACT

Titanium nitride (TiN) has been investigated as a heater material for microhotplates and microreactors. TiN is available in many CMOS processes, unlike many other microheater materials. In addition, TiN has a very high melting point (2950 °C) meaning that it is stable up to higher temperatures than platinum (Pt) and polysilicon. For the first time, TiN is tested inside a conventional membrane of LPCVD silicon nitride (SiN). Two types of sputtered TiN are considered: high stress and low stress. Their performance is compared with that of e-beam evaporated Pt. The maximum average temperature of TiN heaters is 11% higher than those of Pt, and reaches over 700 °C. Failure of the TiN heaters is due to rupture of the membrane. Failure of the Pt heater is due to electro-stress migration. For high-stress TiN, the temperature coefficient of resistance is almost constant and close to that of Pt, making the material very suitable for temperature sensing. In the case of low-stress TiN the temperature coefficient of resistance (TCR) becomes nonlinear and changes sign. The large differences between the materials are explained by the grain structure. The different grain structures are related to the sputtering parameters according to the Thornton model.

Keywords: TiN, Pt, Heater, Microhotplates

1. Introduction

MEMS microhotplates generate high temperatures at low power consumption and exhibit a fast thermal response time. For this reason, they are often used for gas sensors [1,2], membrane-type microreactors [3–9], materials characterization [6–8], and infrared emitters [1,10]. A microhotplate generally consists of a thin film heater coil, wire, or meander which is suspended within a silicon rim for thermal isolation. Often, the heater is supported by a membrane containing low-stress silicon nitride (SiN). The average temperature of the heater is determined from the change of the electrical resistance of the heater or of an additional wire used as temperature sensor.

A popular material for hotplate heaters is platinum (Pt) [2,4,10–14]. This metal can handle large current densities, is highly resistant against oxidation, and can operate up to 550–600 °C without structural changes [4]. It has a melting point of 1768 °C. In addition, it is very suitable for temperature sensing because of its stable temperature coefficient of resistance (TCR). The disadvantages of Pt are its temperature limit, and the fact that it is nonstandard in CMOS fabrication technology.

For these reasons, hotplate heaters have been developed from various other materials to have a complete compatibility with CMOS processes or to increase the temperature of operation of hotplates for applications in micro-reactors, micro-SOFCs and micro-IR emitters for instance. Different materials available in CMOS processes have been evaluated until now as heating elements. The most obvious material that was first used as heater was polysilicon (poly-Si) [1,15,16]. Poly-Si is useful up to 550 °C, above which its resistivity becomes unstable [17,18]. Lately, heaters based on monocrystalline silicon were developed for CMOS hotplates but these MOSFET type heaters still suffer of a lack of stability at high temperature [19,20]. Heaters for higher temperatures, up to 1000 °C, have been made of tantalum silicide (Ta_5Si_3) [21]. Work has been also reported on the use of tungsten based heaters in a SOI technology with satisfying results for the operation of hotplates for metal-oxide gas sensors (300–500 °C) but limitations in their stability when operated at temperatures higher than 600 °C [22,23]. However, this material is not so widely available. It is possible to reach over 1000 °C by using tin oxide doped with antimony [24], and by poly-SiC [25]. Unfortunately, those materials are still nonstandard in CMOS technology.

As an alternative material, we have investigated titanium nitride (TiN) [26]. Thin layers of TiN are widely used in CMOS metallization processes as a diffusion barrier, so the tools for deposition are

* Corresponding author at: DIMES-ECTM (Delft Institute of Microsystems and Nanoelectronics), Delft University of Technology, PO Box 5053, 2600 GB Delft, Netherlands. Tel.: +31 15 2786277.
E-mail address: j.f.creemer@tudelft.nl (J.F. Creemer).

widely available. The element Ti has little or no influence on CMOS transistor operation, even when used in the frond end of the process [27]. In addition, TiN has the potential to reach high temperatures because of its very high melting point (2950 °C for bulk material). It can have a low electrical resistivity (20 μΩ cm [28]), depending on the conditions of deposition. Incidentally, TiN has been used as a heater before [29], but not in hotplates. For this application, TiN has the additional advantage that the residual stress can be tuned over a wide range. This increases the strength of the heater. It also has a very moderate heat conductivity ($15\,W\,m^{-1}\,K^{-1}$ for bulk material). This promises low conductive heat losses through the connecting wires.

This paper presents the fabrication of hotplates with two types of TiN. Their performance is characterized with respect to resistivity, TCR, maximum heater temperature, and response time. The hotplates are compared to Pt hotplates of the same geometry. The observed properties of TiN are related to the deposition conditions and to its grain structure.

2. Design, fabrication, and characterization

The layout of our hotplates is quite classical and is shown in Fig. 1. It consists of a metallic heater coil of 0.33 mm wide and 210 nm thick, which is sandwiched in between a membrane of silicon nitride of 1 mm wide and 1 μm thick. This construction gives an electrical and chemical isolation from the atmosphere. Our reactor application requires a closed membrane and low thermal losses to the rim, so silicon bridges as in [1] are not incorporated. The heater is equipped with four contacts to enable accurate measurement of the resistance and power dissipation of the hot zone. Hotplates of such a design loose heat mainly by natural convection; radiation and conduction are much smaller [30]. This means that the thermal resistance towards the environment depends mainly on the geometry and is quite independent of the heater material.

The hotplates are fabricated on (1 0 0) silicon wafers of 100 mm wide and 525 μm thick. These are covered by 200 nm wet thermal oxide and 500 nm low-stress SiN deposited by LPCVD at 850 °C. The heaters are deposited and patterned, and covered by second layer of 500 nm low-stress LPCVD SiN. Contact holes to the bond pads are opened by plasma etching. On the back side, windows are opened in the nitride to form a mask for etching the silicon substrate. This etch is performed in a solution of potassium hydroxide (KOH, 33 wt.%, at 85 °C) to release the membranes. The result is shown in Fig. 2.

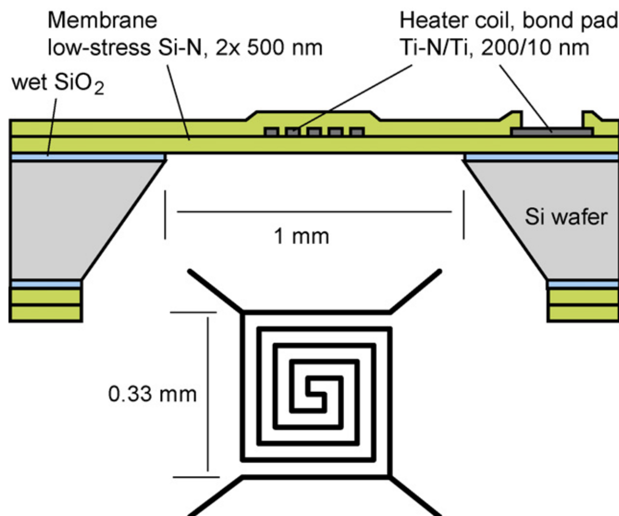

Fig. 1. Schematic cross-section of the hotplates and top view of the heater coil [26].

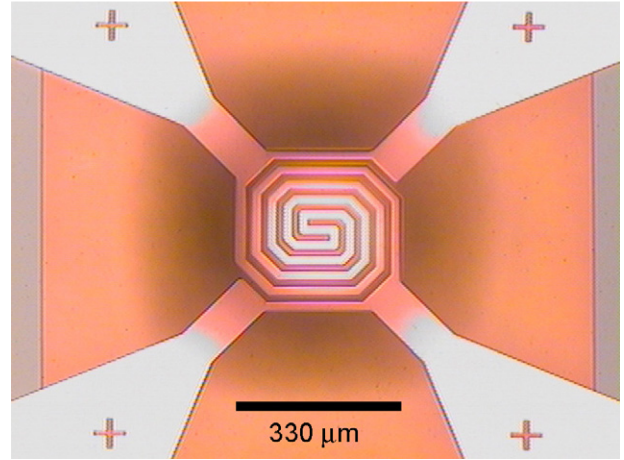

Fig. 2. Pt hotplate during operation under an optical microscope. The shadow is due to thermal buckling [26].

The heaters of TiN are made by reactive sputtering in a Trikon Sigma dc magnetron reactor. The TiN has a thickness of 200 nm and is deposited on 10 nm Ti for a better adhesion to the SiN. Two different types of TiN are sputtered: the standard one with high residual stress, and one with low stress. The major sputtering parameters are given in Table 1. The stress in the TiN is determined from the wafer curvature with a Tencor FLX 2908. The TiN layers are patterned by plasma etching with a chlorine-based chemistry similar to that used for etching aluminum. The contact windows are opened by a plasma etch which is fluorine-based. In both etches, the selectivity is low and an end point detection mechanism is essential. The Pt heaters consist of 185 nm Pt e-beam evaporated on top of a 15 nm Ta adhesion layer. They are patterned using a lift-off process.

The microstructure of the TiN is examined by using an FEI CM30T transmission electron microscope (TEM). The electrical characterization is done with an Agilent 4156C parameter analyzer. With this apparatus, the sheet resistance is measured on Van der Pauw structures. The spirals are heated up to failure by increasing the voltage, in 100 steps of 1 s each. The maximum applied voltages are 14, 100, and 9 V for the heaters of high-stress TiN, low-stress TiN, and Pt, respectively. The temperature of the heaters is estimated from the resistance of Pt and from the power dissipation. It is assumed that the resistance of Pt increases linearly with the temperature, with a TCR of $2.08 \times 10^{-3}\,°C^{-1}$. This value is based on previously calibrated hotplates with the same Pt layer [31,32]. It also corresponds with the experience that Pt thin film heaters start to glow visibly at 600 °C [4]. More accurate measurements could be obtained from experiments in a furnace or on a hot chuck, from IR emission spectroscopy, or by using miniature thermocouples [1,21,33]. The time constant is evaluated by using a waveform generator and an oscilloscope. First, a block-shaped voltage wave of 10 Hz is applied, alternating between 0 V and halfway the maximum input voltage. Meanwhile, the resistance changes are monitored. Second, the small-signal bandwidth is determined by sweeping the

Table 1
Major parameters for sputtering of TiN with high and low residual stress

Parameter	High stress	Low stress
N2 partial pressure (Pa)	0.41	1.8
Total pressure (Pa)	0.53	2.3
Power (kW)	12	0.5
Substrate temperature (°C)	350	350
Bias voltage (V)	0	0

frequency of an AC voltage superposed on a DC voltage of half the maximum input voltage.

3. Results

After deposition the low-stress TiN has a color which is reddish, and the high-stress TiN has a color between gold and copper. The residual stress in the second TiN is compressive and very high: −16.4 GPa. The stress in the other layers is slightly tensile: +0.1 GPa. The high-stress layers are not very well compatible with the remainder of the processing. During the second LPCVD step at 850 °C, they cause blisters and delamination. This has a negative influence on the yield. The two types of TiN show marked differences in the sheet resistances: 2.7 Ω/sq for the high-stress TiN and 0.17 kΩ/sq for the low-stress TiN. The sheet resistance of Pt is 1.4 Ω/sq. The stress value for the Pt after the second deposition of SiN is 1.0 GPa.

During the processing, the TiN must be protected against oxidation. In particular, it should not be heated above 200 °C in an oxygen-containing atmosphere. Also, it should not be cleaned in an RCA SC-1 solution because this is an etchant for Ti and TiN [34]. Finally, it is noticed that the TiN peels of in a KOH solution. The TiN is porous, so that the KOH dissolves the underlying Ti layer.

By applying electrical power, TiN heaters can be brought to emit an intense yellow light; see Fig. 3. The Pt heaters, on the other hand, emit a faint red glow in the dark when heated to the maximum. The resistance changes, power dissipation, and temperatures are shown in Figs. 4 and 5. The maximum values in these figures correspond to the maximum dissipated power before failure. The maximum power of the TiN heaters is 40% higher than that of the Pt heaters. The corresponding temperatures are approximately 720 and 650 °C. Based on these values, the TCR of high-stress TiN is equal to $1.4 \times 10^{-3}\,^{\circ}\mathrm{C}^{-1}$. The increase in resistance with temperature is fairly linear. The low-stress TiN, on the contrary, has a resistance which changes nonlinearly with the temperature. The change even becomes negative at high temperatures. At this stage, no difference in robustness is observed between the high- and low-stress TiN.

When heated to the limit, the TiN and Pt hotplates fail in a different way. This is shown in Figs. 6 and 7. All TiN heaters fail by rupture of the supporting membranes. In addition, they show blisters (delaminations) on the hot parts of the spiral. The blistering is symmetric with respect to the center of the spiral, except for a minor extension onto the two current leading contacts (top right and bottom left). The Pt heaters, on the contrary, do not cause rupture of the membrane. Instead, they show some small blisters on the central, hot area accompanied by staining and roughening of the Pt surface. These observations through the optical microscope are confirmed by inspection in a SEM in backscattering mode. Both the TiN and the Pt heaters fail at a current density of 5×10^5 A/cm^2.

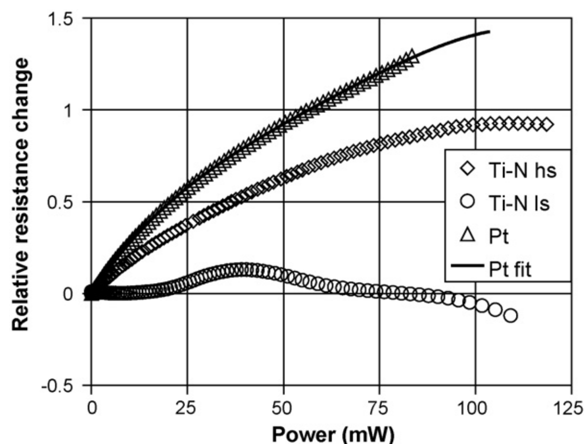

Fig. 4. Resistance change versus dissipated power, for heaters of high-stress TiN (TiN hs), platinum (Pt) and low-stress TiN (TiN ls) [26].

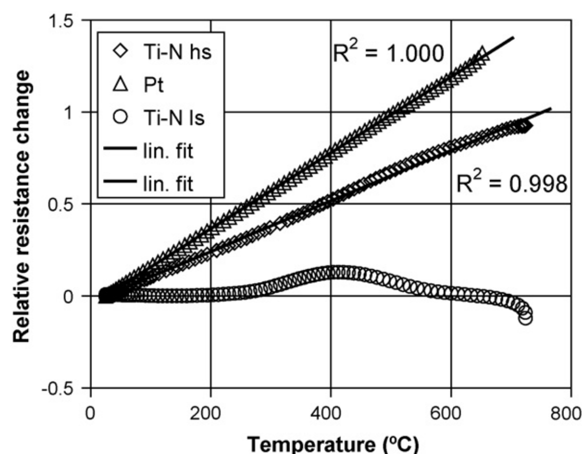

Fig. 5. Resistance change as a function of temperature, for heaters of high-stress TiN (TiN hs), platinum (Pt) and low-stress TiN (TiN ls) [26].

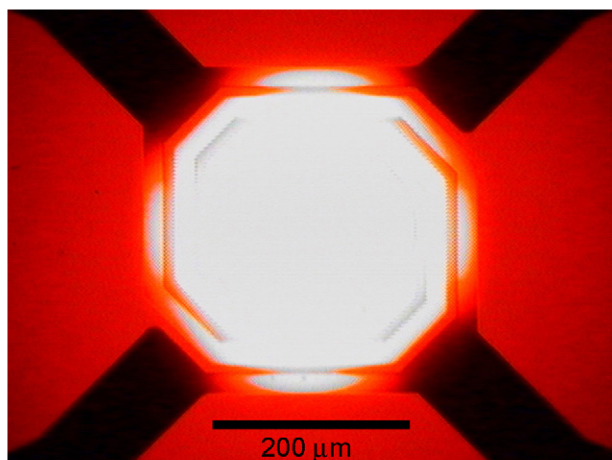

Fig. 3. TiN hotplate during operation at its highest temperature, with the illumination of the microscope turned off [26].

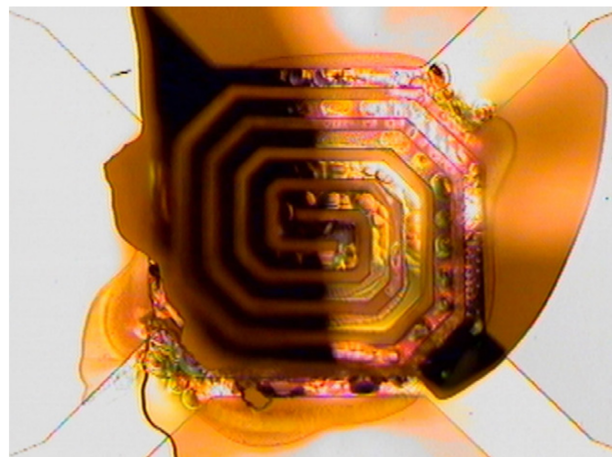

Fig. 6. TiN hotplate after heating up to failure. The membrane is ruptured and the hot parts of the coil are severely blistered.

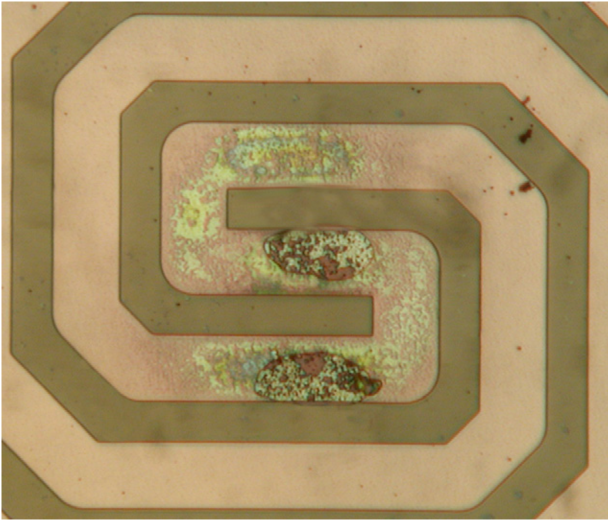

Fig. 7. Central part of a Pt hotplate after heating up to failure. On the hottest area, the SiN cover layer has popped off in two blisters. In addition, the Pt wire is stained and roughened.

The examination with the TEM reveals different grain structures for low- and high-stress TiN. As shown in Fig. 8, high-stress material consists of densely packed fibrous grains with a typical width of 10 nm. The structure corresponds to Zone T of the Thornton classification of sputtered layers [35–37]. Low-stress material, on the other hand, has a porous structure of fibrous grains and contains many voids; see Fig. 9. Dark field images, not shown here, indicate that the grain width is equally around 10 nm. The grain structure corresponds to Zone 1 of the Thornton classification.

The time constant of the step response is 7 ms. The behaviour is that of a first-order system; with our setup no difference can be observed between the heating and the cooling rates. The measured small-signal bandwidth is 3×10^1 Hz. No difference between TiN and Pt hotplates observed, most probably because the thermal resistance is dominated by convection, which is material-independent.

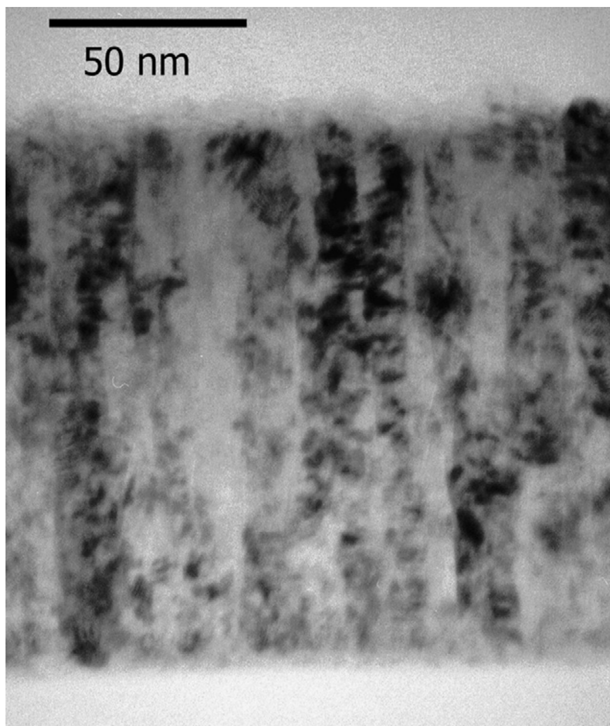

Fig. 8. High-stress TiN layer seen in cross-section by a TEM. The layer consists of long fibrous grains of approximately 10 nm wide [26].

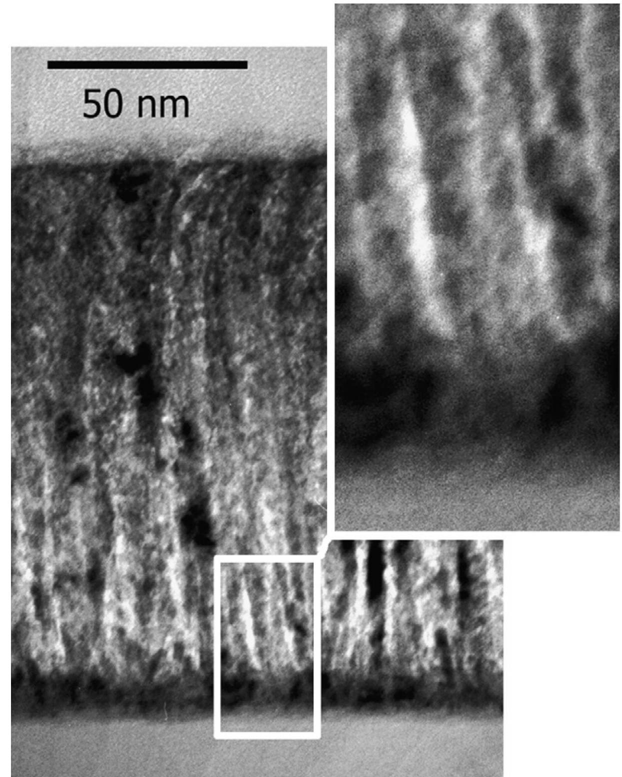

Fig. 9. Low-stress TiN layer seen in cross-section by a TEM. The white stripes are voids between the grains, shown enlarged in the inset [26].

4. Discussion

The colors of the TiN layers indicate that they are both slightly rich of nitrogen [38]. The reddish color of low-stress TiN points towards a higher nitrogen content than the golden-copper appearance of the high-stress material. This can be explained by the relatively high nitrogen pressure during deposition [39]. It also agrees with the resistivity measurements. The resistivity of the high-stress material (57 μΩ cm) is much closer to the minimum value reported in literature (20 μΩ cm [27]) than the resistivity of the low-stress material (3.6 mΩ cm). The minimum in literature was reached only by stoichiometric layers, which are characterized by a yellow golden color. To reach the minimum, the material should also be free of oxygen contamination [39,40]. This can be obtained by applying a bias voltage below −75 V to the substrate. In the sputtering of our TiN no bias voltage has been applied.

High-stress TiN has an appreciable and linear increase in resistivity with temperature, which is interesting for sensing purposes. However, the resistance change of low-stress TiN is fluctuating over the temperature range and is therefore not so useful.

The difference in stress between the TiN layers may be attributed for a part to the influence of 'ion peening'. This is the ion bombardment during the deposition causing a pressure and therefore a residual stress in the layer. Low-stress TiN is sputtered at a much lower power than high-stress TiN. Consequently, it grows under a much lighter bombardment of ions [41].

To a large extent, however, the differences in layer properties can be explained from the difference in morphology of the grain structures. The voids in the Zone 1 material absorb residual mechanical stress. In addition, they are strong scatterers for electrons, which increases the resistivity. Also, they can act as energy barriers for electrons traveling between grains, which should also increase the apparent resistivity.

In general, the difference between the grain morphologies is introduced during the sputtering by a combination of gas pressure and substrate temperature [35,36]. A high gas pressure impedes surface diffusion of adatoms. This can be attributed to an increasing oblique component of the incident flux of gas atoms, developing into hemispherical incidence [36]. The limited surface diffusion increases shadowing effects and promotes the creation of voids.

The fact that TiN heaters reach higher temperatures than those of Pt confirms our expectations. These were based on the rule of thumb that above one-third of the melting point the grain boundaries of a material start to diffuse, thereby affecting the mechanical strength and electrical resistance [21]. According to this rule, Pt would be stable up to 400 °C, whereas TiN should work up to 800 °C. The fact that the TiN heaters emit more light is due to their higher temperature, but can also be caused by the difference in emissivity. For the Pt heater the emissivity is 0.1; for the TiN heater it is unknown for the moment. Theoretical predictions are complicated by the transparent coating of SiN, and by the fact that TiN is partially transparent to light, in contrast to Pt. It should also be noted that our hotplate geometry here is not optimized for temperature uniformity, meaning that temperature variations of about 15% can be expected [31].

Failure of the TiN heaters is caused by rupture of the SiN membrane, which is induced by thermal mechanical stress and, probably, a weakening of the SiN strength at higher temperatures. The residual stress plays only a minor role in this process, because the high- and low-stress heaters almost fail at the same dissipated power. Also, the delamination (blistering) seems not to be the primary source of failure, although it certainly shortens the lifetime of the heater by causing stress concentrations and letting in oxygen to the TiN. The delamination is primarily caused by the mismatch in thermal expansion coefficients between the TiN and the SiN. Nevertheless, it may be accelerated by a thinning of the adhesion layer because of diffusion of the Ti atoms. A similar diffusion was observed for Pt/Ta heaters [4].

The Pt/Ta heaters most likely fail due to electro-stress migration of the Pt atoms, which has been observed many times for similar structures and temperatures [1,4,42–44]. Optical and SEM images also point to this cause, although more information could be obtained from cross-sections and an elemental analysis. The observed stains can be attributed to the formation of hillocks and holes in the Pt. These have been observed in the past in Pt/Ta thin films annealed above 550 °C [4]. Such morphology changes are driven by a combination of the elevated temperature and thermal stress. The blistering of the Pt/Ta heater most probably occurs at the interface between the SiN and the Pt. It has been observed in [4] that adhesion of Pt/Ta to SiN remains intact up to 950 °C, whereas the adhesion of just Pt to SiN already degrades at 500 °C.

5. Conclusion

Hotplates of TiN have been fabricated which heat up above 700 °C. The temperature is 11% higher than similar hotplates made of Pt. TiN with high residual stress has a good TCR for temperature sensing, in contrast to low-stress TiN. However, the high stress levels cause yield problems in the fabrication at present. For this type of TiN, work is still to be done to produce layers which are satisfactory in both the TCR and stress. Differences between high- and low-stress TiN are related to the grain structure as well as to the parameters of the sputtering. Low-stress TiN contains many voids. They relax stress but strongly scatter the conduction electrons.

Acknowledgments

We would like to thank the technical staff of the DIMES Technology Centre, Delft University of Technology, and the technical staff of ComLab, the joint IMT-CSEM clean room facility for their support in the fabrication of the devices. We thank Peter Swart for the photographs and the assistance with electrical measurements, Warner Venstra for the assistance with the SEM, and Vassili Svetchnikov for the TEM pictures. We are also grateful to Emile van der Drift, Frans Tichelaar, Patricia Kooyman, Paul Alkemade, and Jan-Dirk Kamminga for the helpful discussions. This research is supported by the Technology Foundation STW, Applied Science Foundation of NWO and the technology programme of the Ministry of Economic Affairs.

References

[1] S. Semancik, R.E. Cavicchi, M.C. Wheeler, J.E. Tiffany, G.E. Poirier, R.M. Walton, J.S. Suehle, B. Panchapakesan, D.L. DeVoe, Microhotplate platforms for chemical sensor research, Sens. Actuators B 77 (2001) 579–591.

[2] I. Simon, N. Barsan, M. Bauer, U. Weimar, Micromachined metal oxide gas sensors: opportunities to improve sensor performance, Sens. Actuators B 73 (2001) 1–26.

[3] R.M. Tiggelaar, P. van Male, J.W. Berenschot, J.G.E. Gardeniers, R.E. Oosterbroek, M.H.J.M. de Croon, J.C. Schouten, A. van den Berg, M.C. Elwenspoek, Fabrication of a high-temperature microreactor with integrated heater and sensor patterns on an ultrathin silicon membrane, Sens. Actuators A 119 (2005) 196–205.

[4] R.M. Tiggelaar, Silicon-based microreactors for high-temperature heterogeneous partial oxidation reactions, Ph.D. dissertation, Univ. of Twente, Enschede, The Netherlands, 2004.

[5] C. Zhang, K. Najafi, L.P. Bernal, P.D. Washabaugh, An integrated combustor-thermoelectric micro power generator, Dig. Transducers '01, Munich, Germany, June 10–14, 2001, pp. 34–37.

[6] D.W. Denlinger, E.N. Abarra, K. Allen, P.W. Rooney, M.T. Messer, S.K. Watson, F. Hellman, Thin film microcalorimeter for heat capacity measurements from 1.5 to 800 K, Rev. Sci. Instrum. 65 (1994) 946–959.

[7] S.L. Lai, G. Ramanath, L.H. Allen, High-speed (10^4 °C/s) scanning microcalorimetry with monolayer sensitivity (J/m^2), Appl. Phys. Lett. 67 (1995) 1229–1231.

[8] D. Barrettino, M. Graf, W.H. Song, K.U. Kirstein, A. Hierlemann, H. Baltes, Hotplate-based monolithic CMOS microsystems for gas detection and material characterization for operating temperatures up to 500 °C, IEEE J. Solid-State Circuits 39 (2004) 1202–1207.

[9] S.B. Schaevitz, A.J. Franz, K.F. Jensen, M.A. Schmidt, A combustion-based MEMS thermoelectric power generator, Dig. Transducers '01, Munich, Germany, June 10–14, 2001, pp. 30–33.

[10] W. Konz, J. Hildenbrand, M. Bauersfeld, S. Hartwig, A. Lambrecht, V. Lehmann, J. Wöllenstein, Micromachined IR Source with excellent blackbody like behaviour, Proc. SPIE 5836 (2005) 540–548.

[11] D. Briand, A. Krauss, B. van der Schoot, U. Weimar, N. Barsan, W. Göpel, N.F. de Rooij, Design and fabrication of high-temperature micro-hotplates for drop-coated gas sensors, Sens. Actuators B 68 (2000) 223–233.

[12] J.M. Gardner, S.M. Lee, P.N. Bartlett, S. Guerin, D. Briand, N.F. de Rooij, Silicon planar microcalorimeter employing nanostructured films, Dig. Transducers '01, Munich, Germany, June 10–14, 2001, pp. 820–823.

[13] A. Friedberger, P. Kreisl, E. Rose, G. Müller, G. Kühner, J. Wöllenstein, H. Böttner, Micromechanical fabrication of robust low-power metal oxide gas sensors, Sens. Actuators B 93 (2003) 345–349.

[14] J. Courbat, D. Briand, N.F. de Rooij, Reliability improvement of suspended platinum-based micro-heating elements, Sens. Actuators A 142 (2008) 284–291.

[15] M. Parameswaran, A.M. Robinson, D.L. Blackburn, M. Gaitan, J. Geist, Micromachined thermal radiation emitter from a commercial CMOS process, IEEE Electron Device Lett. 12 (1991) 57–59.

[16] J. Laconte, C. Dupont, D. Flandre, J.-P. Raskin, SOI CMOS compatible low-power microheater optimization for the fabrication of smart gas sensors, IEEE Sens. J. 4 (2004) 670–680.

[17] M. Ehmann, P. Ruther, M. von Arx, O. Paul, Operation and short term drift of polysilicon-heated CMOS microstructures at temperatures up to 1200 K, J. Microelectron. Microeng. 11 (2001) 397–401.

[18] O. Grudin, R. Marinescu, L. Landsberger, D. Cheeke, M. Kahrizi, Microstructure release and test techniques for high-temperature micro hotplate, in: Proceedings of the IEEE Canadian Conference on Electrical and Computer Engineering, vol. 3, no. 9, May 12, 1999, pp. 1610–1615.

[19] M. Graf, S. Taschini, P. Käser, C. Hagleitner, A. Hierlemann, H. Baltes, Digital MOS-transistor-based microhotplate array for simultaneous detection of environmentally relevant gases, in: Proceedings of the 17th International IEEE Micro Electro Mechanical Conference (MEMS), Maastricht, The Netherlands, January 25–29, 2004, pp. 351–354.
[20] T. Iwaki, J.A. Covington, J.W. Gardner, F. Udrea, C.S. Blackman, I.P. Parkin, SQI-CMOS based single crystal silicon microheaters for gas sensors, in: Proceedings of the 5th IEEE Sensors Conference, Daegu, Korea, October 22–25, 2006, pp. 460–463.
[21] A. Pollien, J. Baborowski, N. Ledermann, P. Muralt, New material for thin film filament of micromachined hot-plate, Dig. Transducers '01, Munich, Germany, June 10–14, 2001, pp. 848–851.
[22] S.Z. Ali, P.K. Guha, C. Lee, F. Udrea, W.I. Milne, T. Iwaki, J. Covington, J.W. Gardner, J. Park, S. Maeng, High temperature SOI CMOS tungsten micro-heaters, in: Proceedings of the 5th IEEE Sensors Conference, Daegu, Korea, October 22–25, 2006, pp. 847–850.
[23] M.S. Haque, K.B.K. Teo, N.L. Rupensinghe, S.Z. Ali, I. Haneef, S. Maeng, J. Park, F. Udrea, W.I. Milne, On-chip deposition of carbon nanotubes using CMOS microhotplates, Nanotechnology 19 (2008) 025607.
[24] J. Spannhake, A. Helwig, G. Müller, G. Faglia, G. Sberveglieri, T. Doll, T. Wassner, M. Eickhoff, SnO_2:Sb—A new material for high-temperature MEMS heater applications: performance and limitations, Sens. Actuators B 124 (2007) 421–428.
[25] L. Chen, M. Mehregany, Exploring silicon carbide for thermal infrared radiators, in: Proceedings of the 6th IEEE Sensors Conference, Atlanta, GA, USA, October 28–31, 2007, pp. 620–623.
[26] J.F. Creemer, D. Briand, H.W. Zandbergen, W. van der Vlist, C.R. de Boer, N.F. de Rooij, P.M. Sarro, MEMS hotplates with TiN as a heater material, in: Proceedings of the 4th IEEE Sensors Conference, Irvine, CA, USA, October 31–November 3, 2005, pp. 300–303.
[27] L.-H. Chang, W.G. Cowden, J. Christiansen, D. Werho, N.D. Theodore, Is Ti contamination in Si wafer processing an issue? J. Electrochem. Soc. 143 (1996) 2353–2356.
[28] N. Kumar, P. Pourrezaei, M. Fissel, T. Begley, B. Lee, E.C. Douglas, Growth and properties of radio frequency reactively sputtered titanium nitride thin films, J. Vac. Sci. Technol. A 5 (1987) 1778–1782.
[29] P. de Moor, A. Witvrouw, V. Simons, I. de Wolf, The fabrication and reliability testing of Ti/TiN heaters, in: Proceedings of the SPIE, vol. 3874, Santa Clara, CA, USA, September, 1999, pp. 284–293.
[30] A. Pike, J.W. Gardner, Thermal modelling and characterisation of micropower chemoresistive silicon sensors, Sens. Actuators B 45 (1997) 19–26.
[31] D. Briand, S. Heimgartner, M.-A. Grétillat, B. van der Schoot, N.F. de Rooij, Thermal optimization of micro-hotplates that have a silicon island, J. Micromech. Microeng. 12 (2002) 971–978.
[32] L. Thiery, D. Briand, A. Odaymat, N.F. de Rooij, Contribution of scanning probe temperature measurements to the thermal analysis of micro-hotplates, in: Proceedings of the International Workshops on Thermal Investigations of ICs and Systems, Therminic 2004, Sophia Antipolis, France, 2004, pp. 23–28.
[33] M. Graf, D. Barretino, M. Zimmermann, A. Hierlemann, H. Baltes, S. Hahn, N. Bârsan, U. Weimar, CMOS monolithic metal-oxide sensor system comprising a microhotplate and associated circuitry, IEEE Sens. J. 4 (2004) 9–16.
[34] S. Verhaverbeke, J. Parker, A model for the etching of Ti and TiN in SC-1 solutions, in: Proceedings of the Science and Technology of Semiconductor Surface Preparation Symposium, MRS Symposium, vol. 477, San Francisco, CA, USA, April 1–3, 1997, pp. 447–459.
[35] M. Ohring, Material Science of Thin Films, Deposition and Structure, Academic Press, San Diego, 2002 (ch. 5).
[36] S. Craig, G.L. Harding, Effects of argon pressure and substrate temperature on the structure and properties of sputtered copper films, J. Vac. Sci. Technol. 19 (1981) 205–215.
[37] J.A. Thornton, Influence of apparatus geometry and deposition conditions on the structure and topography of thick sputtered coatings, J. Vac. Sci. Technol. 11 (1974) 666–670.
[38] M. Wittmer, Properties and microelectronic applications of thin films of refractory metal nitrides, J. Vac. Sci. Technol. A 3 (1985) 1797–1803.
[39] G. Lemperière, J.M. Poitevin, Influence of the nitrogen partial pressure on the properties of D.C.-sputtered titanium and titanium nitride, Thin Solid Films 111 (1984) 339–349.
[40] J.-E. Sundgren, Structure and properties of TiN coatings, Thin Solid Films 128 (1985) 21–44.
[41] F. Vaz, P. Machado, L. Rebouta, P. Cerqueira, Ph. Goudeau, J.P. Rivière, E. Alves, K. Pischow, J. de Rijk, Mechanical characterization of reactively magnetron-sputtereds TiN films, Surf. Coat. Technol. 174/175 (2003) 375–382.
[42] D. Briand, F. Beaudoin, J. Courbat, N.F. de Rooij, R. Desplats, P. Perdu, Failure analysis of micro-heating elements suspended on thin membranes, Microelectron. Reliab. 45 (2005) 1786–1789.
[43] S.L. Firebaugh, K.F. Jensen, M.A. Schmidt, Investigation of high-temperature degradation of platinum thin films with an in situ resistance measurement apparatus, J. Microelectromech. Syst. 7 (1998) 128–135.
[44] D. Briand, S. Heimgartner, M. Leboeuf, M. Dadras, N.F. de Rooij, Processing influence on the reliability of platinum thin films for MEMS applications, MRS Symposium Proc., BioMEMS and Bionanotechnology, vol. 729, San Francisco, CA, USA, April 2002, pp. 63–68.

Biographies

Fredrik Creemer received his M.Sc. degree in electrical engineering from Delft University of Technology, the Netherlands, in 1995. He received the DEA degree in electronics of Université Paris-Sud in 1996. He obtained his Ph.D. degree from Delft University of Technology, the Netherlands, in 2002, on the effect of mechanical stress on bipolar transistor characteristics. He worked for SystematIC Design in 2002 and the Kavli Institute of Nanoscience in 2003. Currently, he works as an Assistant Professor at the Delft Institute of Microsystems and Nanoelectronics (DIMES-ECTM) of Delft University of Technology. His research interests are MEMS microreactors, transmission electron microscopy, and microsystems technology. Dr. Creemer received the Else Kooi Award 2002 and a Veni grant in 2006.

Danick Briand received his B.Eng. degree and M.A.Sc. degree in engineering physics from École Polytechnique in Montréal, in collaboration with the Laboratoire des Matériaux et du Génie Physique (INPG) in Grenoble, France in 1995 and 1997, respectively. He obtained his Ph.D. degree in the field of micro-chemical systems from the Institute of Microtechnology, University of Neuchâtel, Switzerland in 2001, where he is currently a project leader. He is in charge of European and industrial projects and of the supervision of doctoral students. His research interests in the field of microsystems include PowerMEMS, polymeric MEMS, the integration of nanostructures on microsystems, and the development of micro-analytical instruments for gas-sensing applications.

Henny Zandbergen is full professor in electron microscopy and authored and co-authored about five hundred refereed papers.

Nicolaas F. de Rooij received a Ph.D. degree from Twente University of Technology, The Netherlands, in 1978. From 1978 to 1982, he worked at the Research and Development Department of Cordis Europa N.V., The Netherlands. In 1982, he joined the Institute of Microtechnology of the University of Neuchâtel, Switzerland (IMT UNI-NE), as professor and head of the Sensors, Actuators and Microsystems Laboratory. Since October 1990 till October 1996, he was acting as director of the IMT UNI-NE. Since 1987, he has been a lecturer at the Swiss Federal Institute of Technology, Zurich (ETHZ), and since 1989, he has also been a professor at the Swiss Federal Institute of Technology, Lausanne (EPFL). His research activities include microfabricated sensors, actuators and microsystems.

Pasqualina M. Sarro (M'84-SM'97) received the Laurea degree (*cum laude*) in solid-state physics from the University of Naples, Italy, in 1980. In 1987, she received the Ph.D. degree in electrical engineering from the Delft University of Technology, The Netherlands, her dissertation was dealing with infrared sensors based on integrated silicon thermopiles.

From 1981 to 1983, she was a Postdoctoral Fellow in the Photovoltaic Research Group of the Division of Engineering, Brown University, providence, RI, where she worked on thin-film photovoltaic cell fabrication by chemical spray pyrolysis. Since 1987, she has been with the Delft Institute of Microelectronics and Submicron technology (DIMES), at the Delft University, where she is responsible for research on integrated silicon sensors and MEMS technology. In April 1996, she became Associate Professor in the Electronic Components, Technology and Materials Laboratory of the Delft University and in December 2001 Full Professor in the same department. She has authored and co-authored more than 300 journal and conference papers. In 2004 she received the *Eurosensors Fellow Award* for her contribution to the field of sensors technology.

Dr. Sarro has served as Technical Program Committee member of the ESSDERC Conference (from 1995 till 2002), Eurosensors Conference (since 1999) and IEEE-MEMS 2006. She acted as Technical Program co-chair for the First IEEE Sensors Conference (2002) and as Technical Program Chair for the Second and Third IEEE Sensors Conference (2003 and 2004). Since 2005 she is also AdCom member of the IEEE Sensor Council.